V International Conference on Particle-based Methods – Fundamentals and Applications
PARTICLES 2017
P. Wriggers, M. Bischoff, E. Oñate, D.R.J. Owen, & T. Zohdi (Eds)

IDENTIFICATION OF BLOCK-LIKE MOVEMENT IN COHESIVE AND NON-COHESIVE SPOUTED BED OPERATIONS

ALIJA VILA[1], THOMAS LICHTENEGGER[2], STEFAN PUTTINGER[2] AND STEFAN PIRKER[2]

[1] K1-MET Metallurgical Competence Center (K1-MET)
4020 Linz, Austria
alija.vila@k1-met.com, www.k1-met.com

[2] Department of Particulate Flow Modelling (PFM), Johannes Kepler University (JKU)
4040 Linz, Austria
www.jku.at/pfm

Key words: Gas-solid flows, Spouted bed, Cohesive particles, CFD-DEM

Abstract. Spouted beds are widely used in the chemical and process industries for a large variety of processes. Good understanding of the transport phenomena in these systems is of great importance to improve the design and scale-up procedure [1]. Gas-solid flow heterogeneities, such as particle clustering can have a significant impact on interphase transport properties. The focus of the research is on the interaction between solid particles and interstitial gas. The investigation is realized by means of non-resolved CFD-DEM simulation and the experimental measurement of the spouted bed.

Experimental measurements are conducted in a lab-scale pseudo-2D spouted bed test facility. The cohesive material is substituted by non-cohesive particles with an added moister. With wet particles, it is expected to observe the effects related to the particle cohesion, such as channeling and formation of particle clusters. The main purpose of the experiment is to obtain the information on the overall dynamics of the spouted bed in cohesive and non-cohesive flow regimes. The recorded images were processed with DaVis Particle Image Velocimetry (PIV) post-processing tool.

Numerical CFD-DEM model is developed to investigate the behavior of non-cohesive particles in a spouted bed. Particles are modeled with the Discrete Element Method (DEM), where one integrates Newton's law of motion for each particle under the forces due to the surrounding particles. This method is based on the use of an explicit numerical scheme in which the interaction of the particles is monitored contact by contact [2, 3]. Coupled CFD-DEM simulations allow the incorporation of single-particle properties and modifications of their interaction and as such are suitable for this study. Numerical simulation can be validated by the experimental measurement. Future work will deal with cohesive forces between the particles.

1 INTRODUCTION

Fluidized and spouted beds have a wide industrial application such as drying, combustion, granulation, gasification, coating etc. These applications take advantage of useful properties such as good solid-fluid contact characteristics. While the conventional fluidized bed uses a porous plate distributor, typical spouted bed generally involves a single central orifice. A narrow jet is injected through the orifice which leads to a flow pattern with two distinct regions: a dilute region with upward fluid and particle movement and a dense region including slower downwards moving particles. A spouted bed can operate with larger particle size and more predictable particle circulation compared to a fluidized bed [4].

In industrial applications, cohesion between the particles is a very common occurrence. Cohesive effects lead to the formation of heterogeneities in the particle distribution. In rapid distortion regime of non-cohesive powders with instantaneous inter-particle collisions, such heterogeneities might establish in the form of particle clusters. In cohesive powders where long enduring inter-particle contacts prevail, it might lead to a formation of block-like structures divided by gas tunnels.

Experimental studies conducted by a number of researchers had shown liquid bridge forces having considerable effects on the flow behavior. These studies found that effects of liquid phase include a decrease of the minimum spouted velocity, changes of flow patterns and pressure drop [5, 6, 7].

Due to the difficulties in measurement and control of the cohesive force experimentally, there is a motivation to approach the issue by means of numerical simulation. Coupled approach of CFD and DEM can provide detailed information about behavior on the particle scale. As such, numerical simulations can give valuable information in the analysis of the cohesive effects and their influence on highly dynamic particulate flows [1, 2, 3].

2 PHYSICAL MODELING

Experimental measurements are conducted in a lab-scale pseudo-2D spouted bed test facility. The bed column has a cross section of 150 mm x 20 mm. To allow flow visibility, the column is made of glass front and back plates with aluminum side walls. Air inlet in located in the center of the bed with the width over the whole bed depth. Particles used in the experiment are soda-lime glass spheres, with 2 mm mean diameter and bulk density of 1.5 kg/dm^3. Thus, they belong to particle type D of Geldart classification. Background illumination is achieved with five fluorescent tubes behind the diffusing plate and it provides a good contrast between the particles and the gas phase.

Images are recorded with a Photron Fastcam at 250 frames per second at the resolution of 640 x 928 pixels and exposure time of 1/500 s. The setup allows 9.66 seconds of measurement and results in 2403 images before the internal memory of the camera is full. For each experimental run, an initial snapshot of the bed is captured and initial bed height is calculated. For more details on the set-up, one can refer to the previous work

on flow regime detection in spout-operated fluidized beds [8].

Deionized water is added and mixed with the particles prior to the insertion in the column. Such practice can not ensure the information about the exact amount of the moisture, or the distribution inside the bed. Due to the unsteady nature of the experiment, the water drops would have to be continually added to achieve a steady state. However, this setup should be sufficient as the measurement time is less than 10 seconds, so the change in the moisture content is negligible.

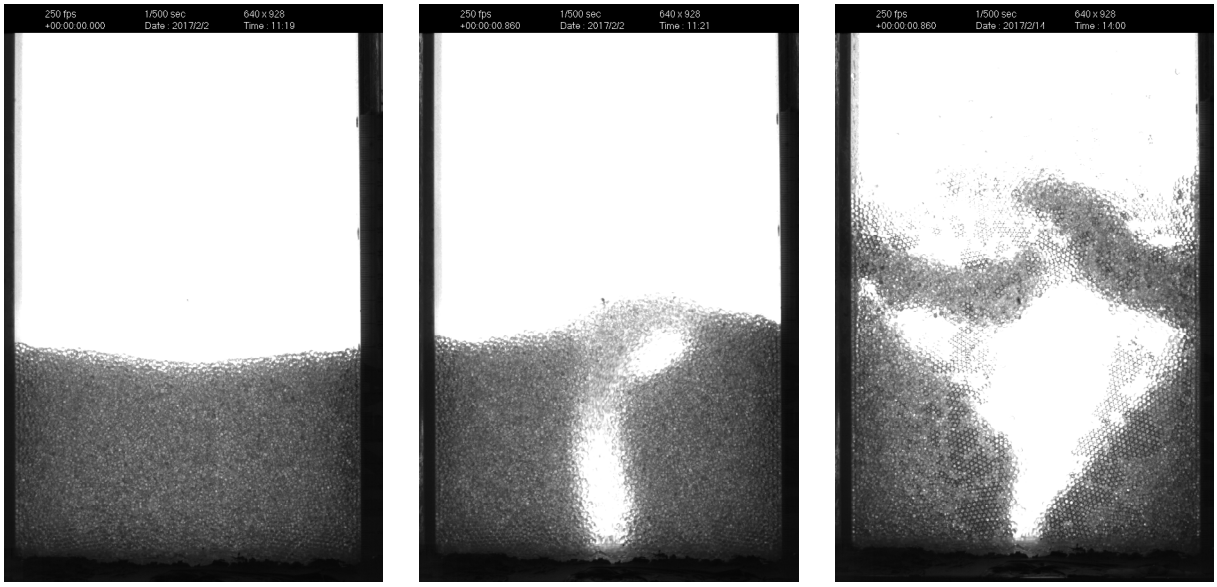

(a) Initial bed configuration (b) After 0.86 s with dry particles (c) After 0.86 s with wet particles

Figure 1: High-speed camera snapshots

Digital image post-processing is done in MATLAB to obtain the mean image and pixel variance image from the series of recorded snapshots. These images provide a reproducible result that can be compared with previous measurements. Image processing also allows the identification of different zones inside the bed. In the mean images, it is possible to observe central spout, blurred moving annulus region, and sharp dead zones.

Since the particles in question are of type D, with relatively large diameter, PIV method can be applied to investigate the particle phase dynamics. The results of tracking algorithm represent the velocity field of the particles phase [9]. Multi-pass PIV time series operation was performed on a windows sizes of 128x128 and 32x32 with an overlap of 50% and 70%, respectively. The geometric mask is defined to avoid the unphysical vectors appearance on the edges and algorithmic thresholding mask to increase the contrast between the fluid and particle phase.

3 NUMERICAL MODELING

In the CFD-DEM model, the gas-phase dynamics are obtained from the volume-averaged Navier-Stokes equations in Computational Fluid Dynamics (CFD) method. The motion of every individual particle is calculated from Newton's second law in the Discrete Element Method (DEM) [1].

3.1 Fluid phase

The equation for mass and momentum conservation are used to compute the motion of the fluid and are given by:

$$\frac{\partial}{\partial t}(\varepsilon\rho_f) + \nabla\cdot(\varepsilon\rho_f\vec{u}_f) = 0 \tag{1}$$

$$\frac{\partial}{\partial t}(\varepsilon\rho_f\vec{u}_f) + \nabla\cdot(\varepsilon\rho_f\vec{u}_f\vec{u}_f) = -\varepsilon\nabla p + \nabla\cdot(\varepsilon\bar{\bar{\tau}}) + \vec{F}_d + \varepsilon\rho_f\vec{g} \tag{2}$$

where ε is the void fraction, ρ_f is the fluid density, $\vec{u}_f$ is the fluid velocity, p is the static pressure, $\bar{\bar{\tau}}$ is the fluid viscous stress tensor, $\vec{F}_d$ is the drag force between the particles and fluid and $\vec{g}$ is the gravitational acceleration. Correlation obtained from Lattice-Boltzmann Method (LBM) was used for the drag force [10].

3.2 Particle phase

Newton's second law of motion is solved for each particle separately in the DEM calculation. Particles are modeled as spheres that interact with each other and the surrounding fluid:

$$m_i\frac{d\vec{v}_{p,i}}{dt} = \vec{F}_i^{(p-p)} + \vec{F}_i^{(p-f)} + \vec{F}_i^{e} \tag{3}$$

where $\vec{F}_i^{(p-p)}$ is the particle-particle contact force, $\vec{F}_i^{(p-f)}$ is the force related to the interaction of particles with a fluid, as the drag force and the pressure gradient.

The force on the particle i due to the surrounding particles j have normal $\vec{F}_{i,j}^{(n)}$ and tangential $\vec{F}_{i,j}^{(t)}$ component described with spring-dashpot model [2].

$$\vec{F}_i^{(p-p)} = \sum_{j\neq 1}(\vec{F}_{i,j}^{(n)} + \vec{F}_{i,j}^{(t)}) \tag{4}$$

Granular hooke/stiffness model is included to describe contact forces between particles. When the distance between the particles is less than their contact distance (sum of two particle diameters), the correlation for the frictional force between two granular particles is used.

$$\vec{F} = (k_n\vec{\delta}_{n_{ij}} - \gamma_n\vec{v}_{n_{ij}}) + (k_t\vec{\delta}_{t_{ij}} - \gamma_t\vec{v}_{t_{ij}}) \tag{5}$$

where $\delta_{n_{ij}}$ is the overlap distance of two particles, k_n the elastic constant for normal contact, k_t the elastic constant for tangential contact, γ_n the viscoelastic damping constant for normal contact, γ_t the viscoelastic damping constant for tangential contact, $\delta_{t_{ij}}$ the tangential displacement vector between two spherical particles, $v_{n_{ij}}$ the normal component of the relative velocity of the two particles and $v_{t_{ij}}$ is the tangential component of the relative velocity of the two particles. The coefficients k_n, k_t, γ_n, γ_t are calculated from the material properties.

3.3 Model setup

The simulation is set up with the geometry and conditions similar to the one in the experiment. The geometry of the modeled pseudo-2D spouted bed matches the test facility cross-section of 150 mm x 20 mm, and a cross-section of 2 mm x 20 mm. The size of the grid must be sufficiently fine to obtain accurate fluid field, but also coarse enough since non-resolved CFD-DEM requires cell larger than particles [13, 14, 15, 16]. The width of the orifice matches the size of the smallest cell in the domain with 2 mm, what is also the size of a single particle. Due to the limitations of the CFD-DEM method, it is not possible to use a finer grind on the inlet for the particles in question. The domain is discretized into 35 x 110 x 6 cells with expansion ratios, as shown in Figure 1.

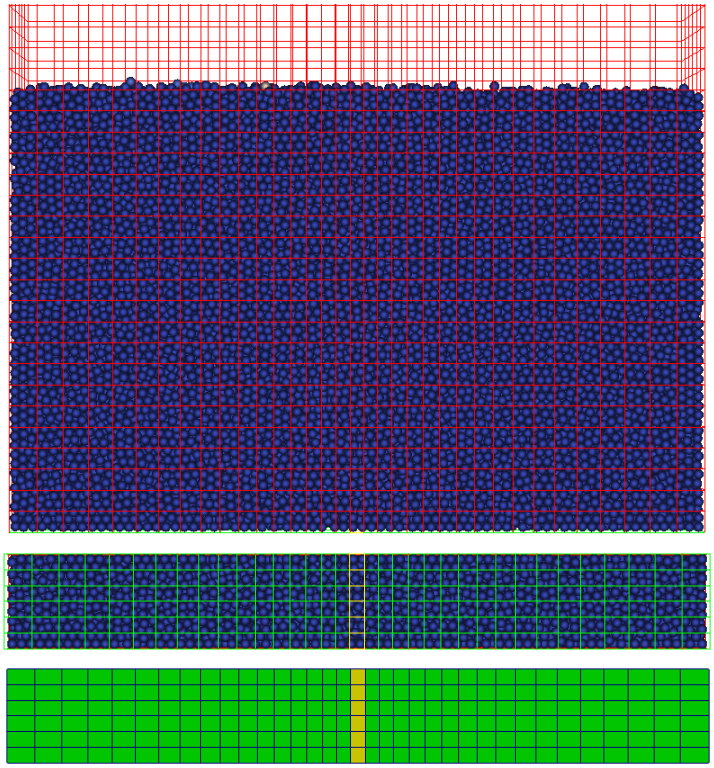

Figure 2: Numerical grid. Front wall and inlet views.

Physical and numerical parameters are defined for two types of the wall so that the particle-wall properties can be modified for sapphire glass front and back wall and aluminum side walls. For additional details on simulation parameters and operating conditions, one can refer to a previous work on CFD-DEM fluidized bed simulation [13].

For particle Reynolds number over 1000, the minimum fluidization velocity can be expressed as [4]:

$$U_{mf}^2 = \frac{d_p(\rho_p - \rho_f)g}{24.5\rho_f} \tag{6}$$

Equations (1), (2) are solved with the PISO algorithm [11] for incompressible flow. Equation (3) is solved with Verlet integration [12] with DEM.

Solid particles are randomly generated with an established mass rate and allowed to settle under gravity to initial bed height $H_0 = 100$ mm. The total number of inserted particles is 42016. With the insertion done, the restart file is created and coupled CFD-DEM simulation can be run. A gas flow is introduced from the inlet with a velocity of $U_{in} = 85$ m/s. On the walls, zero pressure gradient boundary condition is applied, with velocities fixed at 0 m/s. Fixed atmospheric pressure is applied to the outlet. Coupled CFD-DEM simulation of the spouted bed is carried out for 10 seconds of real time what matches the experimental investigation.

4 RESULTS

There is a noticeable visual difference between the results obtained for cohesive and non-cohesive particle-gas flow regimes. Dry particle experiment showed spouted bed behavior with periodic jet fluctuations. Interstitial liquid adds cohesion to the particles, what leads to the formation of channels and fluid flows through preferred path. The movement of the spout it very limited compared to the case with dry particle and observed velocities are lower. The height of the expanded bed is larger with wet particles and bigger void can be observed inside the bed.

It should be noted that particles moving in the dilute spout region might not be detected with the camera, even with chosen low exposure time. Vector values obtained by the post-processing PIV multi-pass time series operation show the dynamics of the dense annular region, fountain and bed surface regions.

Every fourth recorded image is exported to DaVis PIV post-processing tool and the time-step between images is adjusted accordingly. The software gives values for 8960 vectors in each of the 600 frames, resulting in a 3D matrix with dimensions 80x112x600. The results are exported to MATLAB where further post-processing is done in order to find a quantifiable difference between cohesive and non-cohesive particle-gas flows.

The results are analyzed with histogram distribution divided into 100 bins. Values outside of the particle bed are filtered out in order to reduce a redundant number of zero velocity vectors. However, most of the values fall into low-velocity range and in Figure 5. bar graphs are plotted with logarithmic y-axis for better transparency. Histograms

are standardized with a total number of obtained values to compare the two cases. The comparison is made for two parameters: total magnitude and the horizontal component of velocity vectors. Measurements of the dry particle-gas flow gave a wider range of the velocities and more uniform distribution.

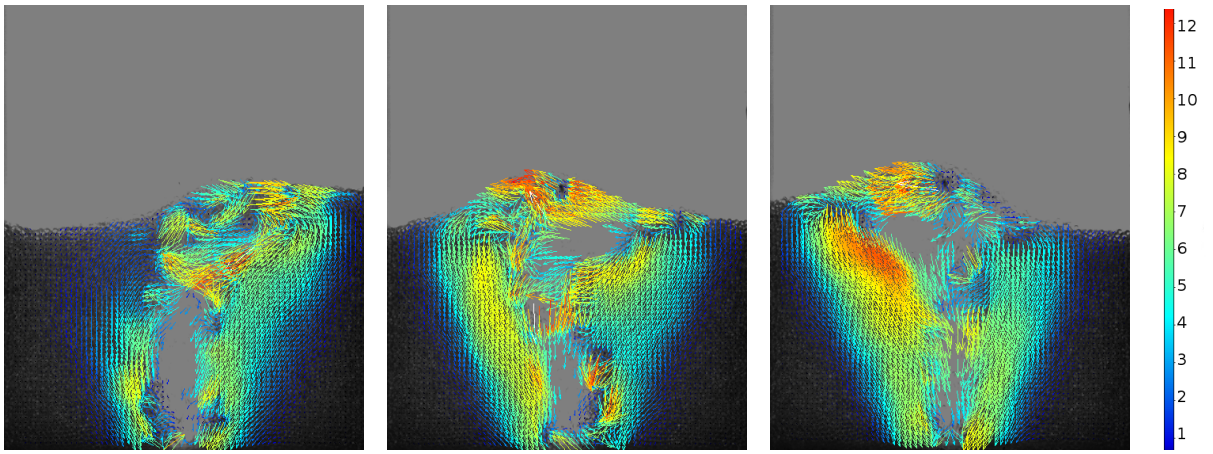

Figure 3: PIV post-processing snapshots for dry particle experiment. The observed pixel displacement range is shown in the scale.

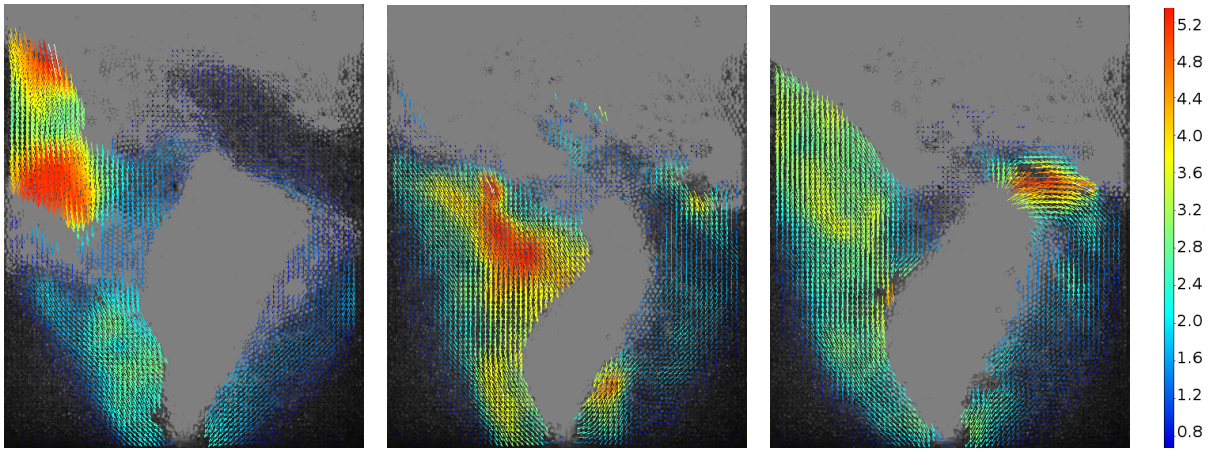

Figure 4: PIV post-processing snapshots for wet particle experiment. The observed pixel displacement range is shown in the scale.

The histogram distribution is made for total velocity magnitude U and horizontal component of the velocity U_x. One bin represents the values in range of 0 - 1.4 px/s and 0 - 0.75 px/s, respectively. The number of vectors inside each bin is tracked for all the processed frames. Autocorrelation process is applied to vector count function for further investigation of the distinct regimes. It was expected to detect a significantly

different time lag of the function before crossing the 0 value. The manner in which the autocorrelation function approaches the 0 value shows some distinctive features for both regimes. However, the difference between sample autocorrelation of the function through the first bin is not too prominent. It should be noted that the investigated function of vector count in the middle of the range for dry particle bed has very strong fluctuations, so autocorrelation process does not result in a clear figure.

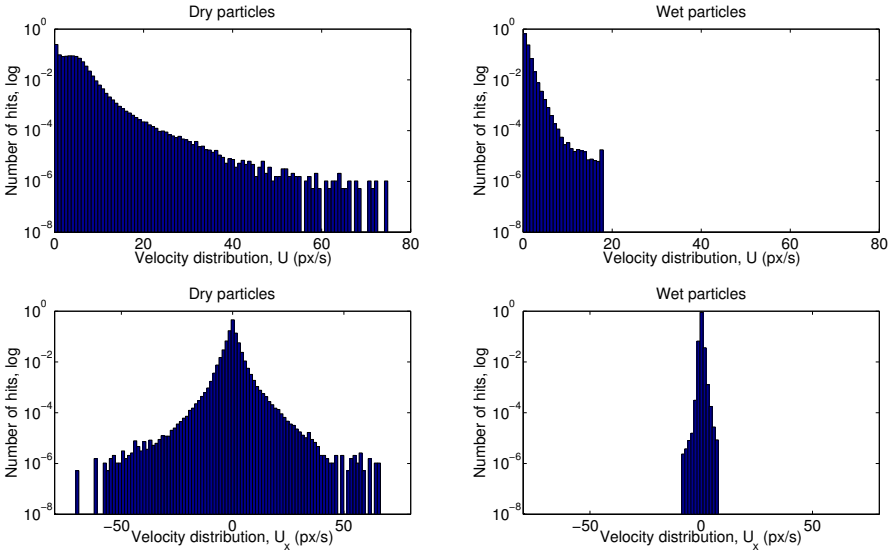

Figure 5: Histogram distribution of the velocity ranges for both regimes.

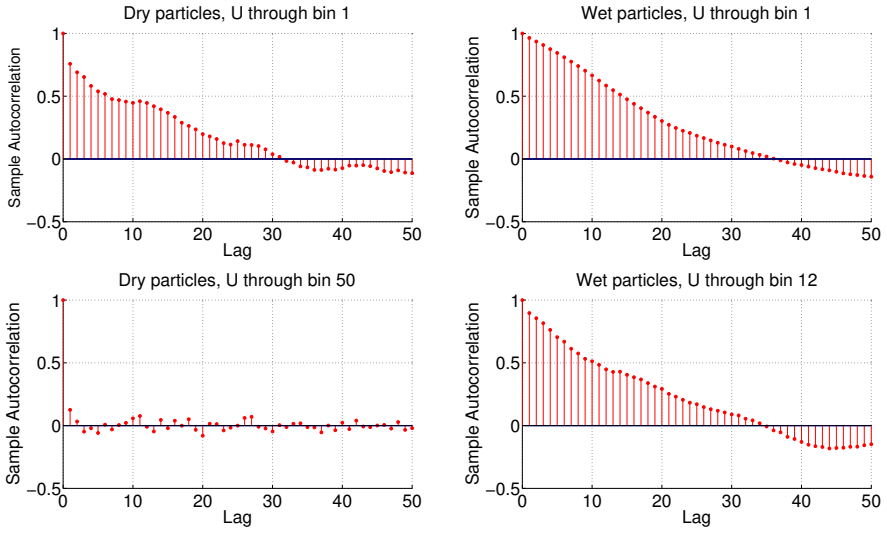

Figure 6: Autocorrelation function of the vector number through 50 frames.

With autocorrelation function not showing a sufficiently clear difference between the cohesive and non-cohesive experiment, a different method has to be applied. Intersections between two functions are tracked to better capture the parameters related to cohesive flow structures. One function being the mean number of vectors in the chosen bin and the other one a number of vectors per frame.

A number of consecutive frames between the intersections can be related with a block-like movement. There is a noticeable difference in chosen parameters obtained from dry and wet particle experiment. A relative number of intersections between referred functions was significantly lower in the cohesive particle-gas flow, with a higher mean number of consecutive frames between intersections.

Table 1: Parameteres related to a block-like movement.

Function	Relative number of intersections	Frames between intersections (mean)
Vectors in first bin (dry)	0.18	5.52
Vectors in middle bin (dry)	0.42	2.36
Vectors in first bin (wet)	0.035	26.14
Vectors in middle bin (wet)	0.12	8.28

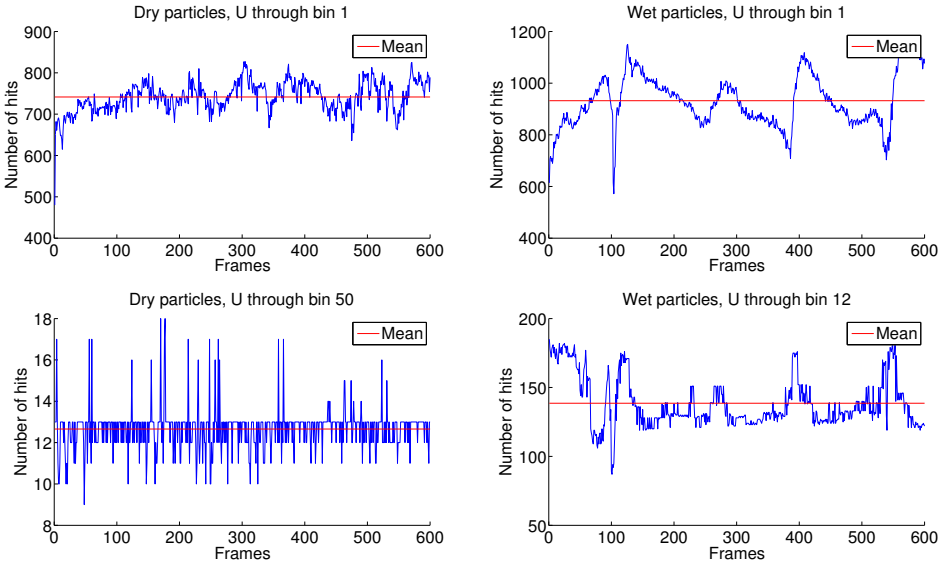

Figure 7: Number of vectors inside the first and the middle bin through the processed frames. Middle of velocity range is represented by the bin number 50 for the dry particles and the bin number 12 for the wet particles.

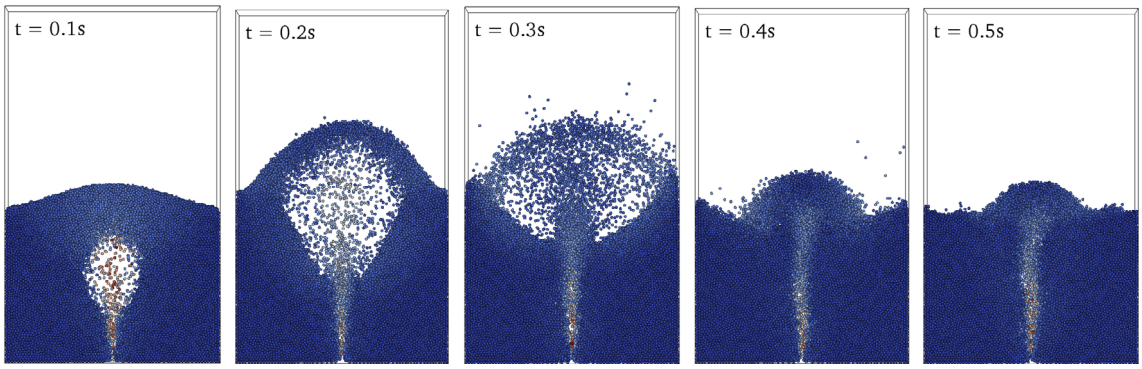

Figure 8: Expansion of a spouted bed predicted by the numerical simulation.

Dry particle experiment can serve as a good validation of the described CFD-DEM model since it is conducted under very similar conditions. The snapshots in Figures 8. and 9. show values of the void fractions inside the bed and the particle velocities. The simulated flow pattern is in good agreement with experimental measurement. As demonstrated, current simulation can predict the behavior of non-cohesive particles in the spouted bed.

Previously described post-processing procedure was applied to images obtained by the numerical simulation. Processed data were compared with the experimental results and good agreement can be found with similar parameters related to a block-like movement.

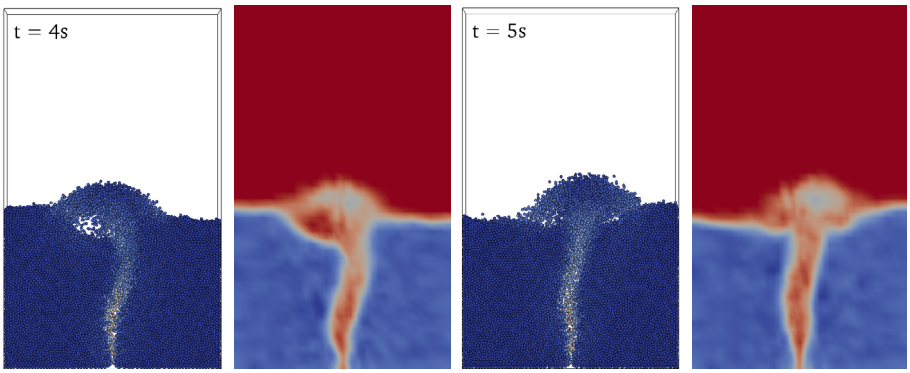

Figure 9: Development of a spouted bed predicted by the numerical simulation.

5 CONCLUSION AND OUTLOOK

In the paper, experimental set-up and post-processing methods are described, together with a developed CFD-DEM spouted bed simulation. The goal of the experiment was to investigate the influence of particle cohesion on the flow behavior. In order to obtain an indicator for block-like movement related to particle cohesion, a new methodology was developed. Non-cohesive particle experiment also serves as a validation of the numerical model.

The experimental measurement showed a significant difference in the solid-gas flow dynamics between the setups with cohesive and non-cohesive particles. Particle image velocimetry operation provided velocity vector values that show the difference between the regimes. Block-like movement of the cohesive particles was detected with PIV method and quantified with post-processing scripts.

The developed CFD-DEM numerical model showed a good agreement with the experimental results. Future work will deal with cohesive forces between the particles. There have been some proposed models to quantify the cohesive interaction [17]. Furthermore, the goal is to develop a new drag model to address the phenomena of the block-like movements and formation of gas tunnels. Such model should provide realistic results that can give a better comparison with measurements.

6 ACKNOWLEDGEMENT

The authors want to acknowledge the financial support from Austrian Federal Ministry of Economy, Family and Youth, and the Austrian National Foundation for Research, Technology and Development.

REFERENCES

[1] Deen, N.G., Van Sint Annaland, M., Van der Hoef, M.A. and Kuipers, J.A.M. Review of discrete particle modeling of fluidized beds. *Chemical Engineering Science*, 62: 28 44, 2007.

[2] Cundall, P.A. and Strack, O.D.L. A discrete numerical model for granular assemblies. *Geotechnique*, 29(1): 4765, 1979.

[3] Tsuji, Y., Kawaguchi, T. and Tanaka, T. Discrete particle simulation of two-dimensional fluidized bed. *Powder Technology*, 77: 79-87, 1993.

[4] Epstein, N. and Grace, J.R. Spouted and Spout-Fluid Beds: Fundamentals and Applications. *Cambridge University Press*, 2010.

[5] Nagahashi, Y., Epstein, N, Grace. J.R., Asako, Y. and Yokogawa A. Effect of cohesive forces on fluidized and spouted beds of wet particles. *Can. J. Chem. Engi.*, 84: 527-531, 2006.

[6] Passos, M.L. and Mujumdar, A.S. Spouting Enhancement by Addition of Small Quantities of Liquid to Gas-Spouted Beds. *Powder Technology*, 110: 222-238, 2000.

[7] Bacelos, M.S., Passos, M.L. and Freire, J.T. Effect of interparticle forces on the conical spouted bed behavior of wet particles with size distribution. *Powder Technology*, 174: 114-126, 2007.

[8] Puttinger, S., von Berg, L., Schneiderbauer S. and Pirker, S. Bed zone and flow regime detection in spout-operated fluidized beds by digital image processing and pressure probes. *8th World Conference on Experimental Heat Transfer, Fluid Mechanics, and Thermodynamics*, 16-20, 2013.

[9] Puttinger, S., Holzinger, G. and Pirker, S. Investigation of highly laden particle jet dispersion by the use of a high-speed camera and parameter-independent image analysis. *Powder Technology*, 234: 46-57, 2013.

[10] Beetstra, R., Van der Hoef, M.A. and Kuipers, J.A.M. Drag force of intermediate Reynolds number flow past mono- and bidisperse arrays of sphere. *AIChE J.*, 53: 489-501, 2007.

[11] Issa, R.I. Solution of the implicitly discretised fluid flow equations by operator-splitting. *J. Comput. Phys.*, 62: 40-65, 1986.

[12] Verlet, L. Computer "experiments" on classical fluids. I. Thermodynamical properties of Lennard-Jones molecules. *Phys. Rev.*, 159: 98, 1967.

[13] Lichtenegger, T., Peters, E.A.J.F., Kuipers, J.A.M. and Pirker, S. A recurrence CFD study of heat transfer in a fluidized bed. *Chemical Engineering Science*, 2017.

[14] Lichtenegger, T. and Pirker, S. Extremely fast simulations of heat transfer in fluidized beds. *Proceedings of the 12th International Conference on CFD in the Oil & Gas, Metallurgical and Process Industries, Trondheim* , 2017.

[15] Hoomans, B.P.B., Kuipers, J.A.M., Briels, W.J. and van Swaaij, W. Discrete particle simulation of bubble and slug formation in a two-dimensional gasfluidised bed: a hard-sphere approach. *Chemical Engineering Science*, 51: 99-118, 1996.

[16] Link, J., Cuypers, L.A., Deen, N.G. and Kuipers, J.A.M. Flow regimes in a spoutfluid bed: A combined experimental and simulation study. *Chemical Engineering Science*, 60: 3425-3442, 2005.

[17] Xu, H., Zhong, W., Yuan, Z. and Yu, A.B. CFD-DEM study on cohesive particles in a spouted bed. *Powder Technology*, 314: 377-386, 2017.